

Using input warping to improve the Bayesian optimisation of a complex epidemiological model of the sharka virus

Victor Picheny · Coralie Picard · Gael Thebaud

Received: date / Accepted: date

On peut [Victor's comment: faire un commentaire] [Coralie's comment: chacun avec sa couleur], on peut aussi ~~enlever des trucs~~ ou bien ajouter d'autres trucs, et Gael aussi.

Abstract Optimizing mathematical model parameters remains a challenge in many research fields, in particular when these parameters are numerous and when the model result depends on their interaction. In this work, we focus on a Bayesian optimization approach, accounting for the local invariances of the parameters (that means that for some values of a subset of parameters, the model is insensitive to another subset of parameters). To this end, we apply a warping to the parameter space. This approach was tested on a simulation model of sharka disease spread and management. This disease is caused by a virus which induces numerous damages on *Prunus* trees. Specifically, we analyzed the contribution of the warping on the optimization of sharka control options. We show that the final result of the optimization is not impacted by the use of the warping. However, it impacts the optimization speed. Indeed, the optimization process with warping allowed finding the best result faster than without. Such warping process could be used for various optimization issues presenting invariances in order to reduce the calculation time.

Keywords Bayesian optimisation, warping, spatio temporal model, sharka

V. Picheny
MIAT, Université de Toulouse, INRA, Castanet-Tolosan, France
Tel.: +33561285551
E-mail: victor.picheny@inra.fr

C. Picard
BGPI, Montpellier SupAgro, INRA, Univ. Montpellier, Cirad, TA A-54/K, 34398, Montpellier

G. Thebaud
to do

1 Introduction

Mathematical models are increasingly used in many research fields to understand and optimize a process. For instance, they are useful in epidemiology to predict epidemics and to propose efficient control options [4, 5, 16, 31, 1, 12, 32, 9]. However, these epidemiological studies are mostly focused on improving one control option which generally depends on only one or two parameters in their model, although various control actions are usually applied simultaneously to manage an epidemic. All these actions could be jointly optimized but taking into account numerous management parameters in an optimization problem can be difficult, especially when the management efficiency depends on the interaction between these parameters.

In this study, we analyse a simulation model of sharka disease spread and management. This disease, caused by a virus transmitted by aphids through *Prunus* orchard, is one of the most damaging diseases of stone fruit trees belonging to the genus *Prunus* (e.g. peach, apricot and plum) [3, 23]. Our model includes epidemiological parameters which vary between simulations, and various landscapes on which the virus can spread, which means that this model is stochastic. In addition, management parameters allow to simulate orchard surveillance. Here, we aim to optimize these management parameters using an efficient optimization algorithm.

Within the wide range of potential approaches to solve such optimization problems, black-box optimization methods have proven to be popular in this context [26], in particular because they are in essence non-intrusive: they only require pointwise evaluations of the model at hand (output value for a given set of inputs), as opposed to knowing the underlying mechanisms of the model, structural information, derivatives, etc. This greatly facilitates implementation and avoids developing tailored algorithms. In this work, we focus more particularly on the so-called *Bayesian optimization* (BO) approaches [15, 28], which are well-suited to tackle stochastic and expensive models.

In some cases, the user possesses relevant information regarding his model that could facilitate the optimization task. Accounting for this information within a black-box optimization framework (or rather: *grey box*) may be a challenging task as it is, in essence, unnatural. In this work, we focus on a particular type of information, which we refer to as *local invariance*: for some values of a subset of parameters, it is known that the model is insensitive to another subset of parameters. As an illustration, take a function y that depends on two discs, parameterized by $x_1 = r_1 \in [0, r_{\max}]$ (radius of the first disc) and $x_2 = \rho_{12} \in [0, 1]$ (ratio between r_1 and the radius of the second disc, r_2). An action A_1 is conveyed on the first disc and another action A_2 on the second. Setting $x_1 = 0$, we have $r_2 = 0$ for any value of ρ_{12} , so $y(0, x_2)$ is constant.

Intuitively, one may want to rework the definition of the parameters to optimize over in order to remove the invariances. However (as we show in 2), such a reformulation is not always possible. Here, we propose to keep the optimisation problem unchanged, and convey the invariance information to the BO algorithm directly, by applying a *warping* [29, 30] to the parameter space.

The remainder of this paper is structured as follows. Section 2 describes the sharka model and its invariances. Section 3 presents the basics of Bayesian optimization and

our warping strategy. Finally, section 3 analyses the efficiency of the warping on the sharka model.

2 Model description and problem set-up

The simulation model that we analyze in this work is a stochastic, spatially explicit, SEIR (susceptible-exposed-infectious-removed) model that simulates sharka spread and management actions [including surveillance, removals and replantations 20, 24, 25].

This model is orchard-based, with a discrete time step of one week. It allows to perform simulations on landscapes composed of uncultivated areas and patches on which peach trees are grown. The patches can be more or less aggregated in the landscape however, we only use in this work the 30 landscapes with a high level of patch aggregation as described by [17]. During the simulation, the trees in the patches are characterized by different states. When the simulation begins, they are not infected: they are in the “susceptible” state. Then, the virus is introduced the first year of the simulation in one of the patches and spreads through orchards (new introductions can also occur during the entire simulation on all patches). The virus causes changes in tree status: from “susceptible”, they become “exposed” (infected but not yet infectious or symptomatic), “infectious hidden” (after the end of the latent period), “infectious detected” (when specific symptoms are detected on the tree during a survey), and “removed” (when the tree is removed from the patch). The model output is an economic criterion, the net present value (NPV), which accounts for the benefit generated by the cultivation of productive trees and the costs induced by fruit production and disease management [25].

In order to simulate wide range of epidemic and management scenarios, the model includes 6 epidemiological and 23 management parameters [25, 17]. In this work, we will use the 6 epidemiological parameters and only 10 management parameters (related to the surveillance of the orchards). They include distances of 3 zones for which the surveys are more or less frequent as well as their duration, the probability of the infected tree detection, and a contamination threshold which can request to increase the surveillance frequency in the focal zone. Details of management parameters used in this study are presented in Fig.1 and Table 1 (this table also includes the variation ranges of the parameters in the model).

Here, we aim to optimize the management strategy of the disease (i.e. to find the combination of management parameters allowing to obtain the best NPV), taking into account the epidemic stochasticity. However, we note that some combinations of management parameters can represent the same management, which may cause problems in the optimization process. Indeed, we observe that some management parameters are not useful when other parameters have a value of 0, which means that they can take any values without modifying the simulation. For example, when a zone radius is 0, the associated surveillance frequency have no impact on the NPV (regardless its value). The methodological developments that are proposed in this work address this issue by removing the parameter combinations which lead to the

same management. The parameter invariances removed from the model are listed in Table 2.

Table 1 Management parameters implemented in the previously developed model with minimum and maximum values corresponding to the variation range of each parameter.

		Min	Max
ρ	Probability of detection of a symptomatic tree	0	0,66
γ_O	Duration of observation zones (years)	0	10
ζ_s	Radius-distance of security zones (m)	0	5800
ζ_f	Radius-distance of focal zones (m)	0	1
ζ_{eo}	Radius-distance of observation epicenter (m)	0	1
$1/\eta_0$	Maximal period between 2 observations (year)	1	15
η_s	Observation frequency in security zones (year-1)	0	8
η_f	Observation frequency in focal zones (year-1)	0	8
η_{f*}	Modified observation frequency in focal zones (year-1)	0	8
χ_o	Contamination threshold in the observation epicenter, above which the observation frequency in focal zone is modified	0	1

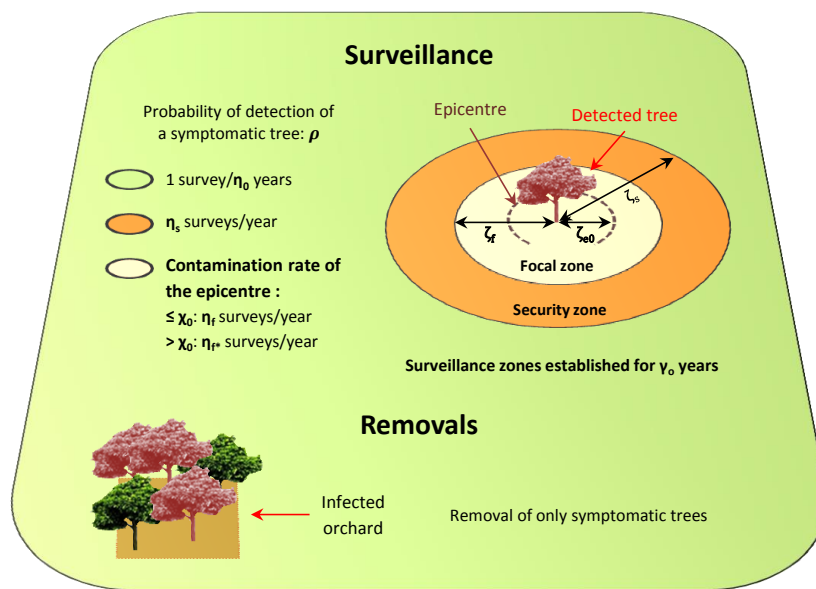


Fig. 1 Management actions implemented in the model.

Table 2 Invariances of management parameters. For instance, when $\gamma_O = 0$ or when $\rho = 0$, χ_o does not influence the model output.

Management parameters	OR	OR	OR
ρ			
$1/\eta_0$			
γ_O			
χ_o	$\gamma_O = 0$ $\rho = 0$		
ζ_{eo}	$\gamma_O = 0$ $\zeta_s = 0$ $\rho = 0$		
ζ_f	$\gamma_O = 0$ $\zeta_s = 0$		
η_{f*}	$\gamma_O = 0$ $\rho = 0$		
ζ_s	$\gamma_O = 0$ $\eta_s = 0$		
η_s	$\gamma_O = 0$		
η_f	$\gamma_O = 0$		

3 Methods: Bayesian optimization

3.1 Overview

Bayesian optimization can be seen as a modernization of the statistical response surface methodology for sequential design [2], where the basic idea is to replace an expensive function by a cheap-to-evaluate surrogate one. In BO, Gaussian process (GP) regression, or kriging, is used to provide flexible response surface fits. GPs are attractive in particular for their tractability, since they are simply characterized by their mean $m(\cdot)$ and covariance (or kernel) $k(\cdot, \cdot)$ functions, see e.g., Rasmussen and Williams [22]. In the following, we consider zero-mean processes ($m = 0$) for the sake of conciseness.

Conditionally on n noisy observations $\mathbf{f} = (f_1, \dots, f_n)$, with independent, centered, Gaussian noise, that is, $f_i = y(\mathbf{x}_i) + \varepsilon_i$ with $\varepsilon_i \sim \mathcal{N}(0, \tau_i^2)$, the predictive distribution of y is another GP, with mean and covariance functions given by:

$$\mu(\mathbf{x}) = \mathbf{k}(\mathbf{x})^\top \mathbf{K}^{-1} \mathbf{f}, \quad (1)$$

$$\sigma^2(\mathbf{x}, \mathbf{x}') = k(\mathbf{x}, \mathbf{x}') - \mathbf{k}(\mathbf{x})^\top \mathbf{K}^{-1} \mathbf{k}(\mathbf{x}'), \quad (2)$$

where $\mathbf{k}(\mathbf{x}) := (k(\mathbf{x}, \mathbf{x}_1), \dots, k(\mathbf{x}, \mathbf{x}_n))^\top$ and $\mathbf{K} := (k(\mathbf{x}_i, \mathbf{x}_j) + \tau_i^2 \delta_{i=j})_{1 \leq i, j \leq n}$, δ standing for the Kronecker function.

Commonly, $k(\cdot, \cdot)$ belongs to a parametric family of covariance functions such as the Gaussian and Matérn kernels, based on hypotheses about the smoothness of y . Corresponding hyperparameters are often obtained as maximum likelihood estimates, see e.g., Rasmussen and Williams [22] or Roustant et al [27] for the corresponding details.

BO typically tackles optimization problems of the form:

$$\begin{aligned} \min \quad & y(\mathbf{x}) \\ \text{s.t. } & \mathbf{x} \in \mathbb{X}, \end{aligned}$$

with $\mathbb{X} \in \mathbb{R}^d$ is usually a bounded hyperrectangle and $y : \mathbb{R}^d \rightarrow \mathbb{R}$ is a scalar-valued objective function.

Optimization amounts here to choosing a sequence of points $\mathbf{x}_{n+1}, \dots, \mathbf{x}_{n+N}$ at which the function y is evaluated. Sequential design decisions, so-called *acquisitions*, are based on the GP model and judiciously balance exploration and exploitation in search for global optima. The GP model is updated after each new value is calculated.

In the noiseless setting ($\tau = 0$), the canonical acquisition function is *expected improvement* (EI) [11]. Define $f_{\min} = \min_{i=1,\dots,n} y_i$, the smallest y -value seen so far, and let $I(\mathbf{x}) = \max\{0, f_{\min} - Y(x)\}$ be the *improvement* at x . $I(x)$ is largest when $Y(\mathbf{x})$ has substantial distribution below f_{\min} . The expectation of $I(x)$ over $Y(x)$ has a convenient closed form, revealing balance between exploitation ($\mu(x)$ under f_{\min}) and exploration (large $\sigma^n(x)$):

$$\mathbb{E}\{I(x)\} = (f_{\min} - \mu(x))\Phi\left(\frac{f_{\min} - \mu(x)}{\sigma(x)}\right) + \sigma(x)\phi\left(\frac{f_{\min} - \mu(x)}{\sigma(x)}\right), \quad (3)$$

where $\Phi(\phi)$ is the standard normal cdf (pdf).

3.2 Bayesian optimization of stochastic simulators

When y is only available through noisy evaluations, the EI acquisition cannot be used directly. Several authors have tackled this issue; we refer to [19] for a review on the topic. We chose here to focus on the *reinterpolation method* proposed in [10], which is based on the use of an instrumental noiseless kriging model, built from the original one. First, the (noisy) kriging predictions at the DOE points $\mu(\mathbf{x}_1), \dots, \mu(\mathbf{x}_n)$ are computed. Then, a reinterpolating model is built, by using the same covariance kernel and parameters and the same experimental design, but the observation vector is replaced by $\mu(\mathbf{x}_1), \dots, \mu(\mathbf{x}_n)$ and the noise variance is set to zero. Since this latter model is noise-free, the classical EI can be used as the infill criterion. Once the new design is chosen and the evaluation is performed, both kriging models are updated. One particular characteristic of this strategy is that it does not allow repetitions, which is desirable in our case.

3.3 Bayesian optimization with invariances

3.3.1 Definition of local invariances

From Section 2, we observe that there are cases of invariances involving a single or several variables. Here, we formalize the different situations and generalize some cases.

We first introduce the following notation (this is purely notation, no actual permutation is performed):

$$y(\mathbf{x}) = y(x_i, \mathbf{x}_J, \mathbf{x}_{-iJ}) \quad (4)$$

$$\mathbb{X} = \{\mathbb{X}_i, \mathbb{X}_J, \mathbb{X}_{-iJ}\} \quad (5)$$

Definition 1 (Simple) We call *simple invariance* the following case: y is invariant with respect to \mathbf{x}_J (J a subset of $\{1, \dots, d\} \setminus i$) if $x_i = c_i$ ($i \in \{1, \dots, d\}$):

$$y(c_i, \mathbf{x}_J, \mathbf{x}_{-iJ}) = y(c_i, \mathbf{x}'_J, \mathbf{x}_{-iJ}), \quad \forall \mathbf{x}_J, \mathbf{x}'_J \in \mathbb{X}_J, \mathbf{x}_{-iJ} \in \mathbb{X}_{-iJ}.$$

This corresponds for instance to the last line of Table 2: the observation frequency η_f does not have an effect on the model if the duration of observation γ_O is set to zero.

Definition 2 (Or) We call “*or*” *invariance* the following case: y is invariant with respect to \mathbf{x}_J (J a subset of $\{1, \dots, d\} \setminus I$) if there exists at least one $i \in I$ such that $x_i = c_i$ (I a subset of $\{1, \dots, d\} \setminus J$):

$$y(c_i, \mathbf{x}_{I \setminus i}, \mathbf{x}_J, \mathbf{x}_{-IJ}) = y(c_i, \mathbf{x}_{I \setminus i}, \mathbf{x}'_J, \mathbf{x}_{-IJ}), \quad \forall \mathbf{x}_J, \mathbf{x}'_J \in \mathbb{X}_J, \mathbf{x}_{I \setminus i} \in \mathbb{X}_{I \setminus i}.$$

This corresponds for instance to the fourth line of Table 2: the contamination threshold in the observation zone ξ_0 does not have an effect on the model if the duration of observation γ_O is set to zero or if the probability of detection ρ is set to zero.

Definition 3 (Linear) We call *linear invariance* the following case: y is invariant with respect to \mathbf{x}_J (J a subset of $\{1, \dots, d\} \setminus I$) if $\mathbf{Ax}_I = \mathbf{b}$, with I a subset of $\{1, \dots, d\} \setminus J$, \mathbf{A} a matrix of size $p \times \text{Card}(I)$ and \mathbf{b} a vector of size p :

$$y(\mathbf{x}_I, \mathbf{x}_J) = y(\mathbf{x}_I, \mathbf{x}'_J), \quad \forall \mathbf{x}_J, \mathbf{x}'_J \in \mathbb{X}_J, \text{ if } \mathbf{Ax}_I = \mathbf{b}.$$

There are two particular cases worth noting:

- setting $p = \text{Card}(I)$, $\mathbf{A} = \mathbb{I}_p$ and $\mathbf{b} = \mathbf{c}_I$ results in an “AND” condition: y is invariant with respect to \mathbf{x}_j if, $\forall i \in I$, $x_i = c_i$;
- setting $p = 1$, $\mathbf{A} = [1, -1]$ results in an invariance under the condition $x_{i1} = x_{i2}$.

3.3.2 Principle of input warping

The standard use of GPs implies a hypothesis of stationarity (the unconditional joint probability distribution of the process does not change when shifted in the \mathbb{X} space), which is in contradiction with the notion of local invariance.

There are several ways of incorporating structural information into Gaussian processes. One is to work on the kernel function k [8, 6]. Another, which is the one we use here, is to transform the original input space \mathbb{X} into a *warped* one $\tilde{\mathbb{X}}$ and index the GP on $\tilde{\mathbb{X}}$, so that the new topology directly reflects the structural information [30, 13].

Consider for simplicity a single invariance over x_J when $x_i = c_i$. A simple way to handle this problem is to distort locally the space so that the subspace $\{(x_i, \mathbf{x}_J) | x_i = c_i\}$ collapses to a single point, for instance with \mathbf{x}_J at its average value: $(c_i, \bar{\mathbf{x}}_J)$.

Hence, we are seeking warping functions of the form:

$$\begin{aligned}\psi : \mathbb{X} &\rightarrow \widetilde{\mathbb{X}} \\ \mathbf{x} &\mapsto \widetilde{\mathbf{x}} = \psi(\mathbf{x})\end{aligned}$$

such that:

1. $\psi(x_i, \mathbf{x}_J, \mathbf{x}_{-iJ}) = (c_i, \overline{\mathbf{x}_J}, \mathbf{x}_{-iJ})$ if and only if $x_i = c_i$;
2. ψ restricted to $\mathbb{X} \setminus (c_i, \dots)$ and $\widetilde{\mathbb{X}} \setminus (c_i, \overline{\mathbf{x}_J}, \dots)$ is a diffeomorphism.

In addition, we will search for deformations that decrease monotonically when $|x_i - c_i|$ increases, that is:

$$\begin{aligned}((x_i, \mathbf{x}_J, \mathbf{x}_{-iJ}), \psi[(x_i, \mathbf{x}_J, \mathbf{x}_{-iJ})]) &\leq d((x'_i, \mathbf{x}_J, \mathbf{x}_{-iJ}), \psi[(x'_i, \mathbf{x}_J, \mathbf{x}_{-iJ})]) \\ \text{if } |x_i - c_i| &\leq |x'_i - c_i|,\end{aligned}$$

for some distance $d(\cdot, \cdot)$.

Since the \mathbf{x}_J dimension collapses to $\overline{\mathbf{x}_J}$ at $x_i = c_i$, we write:

$$\forall j \in J, \quad \widetilde{x}_j = \overline{x}_j + (x_j - \overline{x}_j) \alpha(x_i, c_i), \quad (6)$$

with $\alpha(x_i, c_i)$ an attenuation function such that:

1. $\alpha(c_i, c_i) = 0$;
2. α increases monotonically with $|x_i - c_i|$;
3. $0 < \alpha \leq 1, \forall x_i \neq c_i$.

Condition 1 ensures that $\widetilde{x}_j = \overline{x}_j$ when $x_i = c_i$ (the J -th dimensions collapse).

3.3.3 Warping for a simple invariance

In the simple invariance case, we propose linear and correlation-based attenuation functions:

$$\alpha_{\text{lin}}(x_i, c_i) = \frac{|x_i - c_i|}{\delta_i}, \quad (7)$$

$$\alpha_{\text{cor}}(x_i, c_i) = 1 - r(x_i, c_i), \quad (8)$$

where r is a $\mathbb{R} \times \mathbb{R} \rightarrow \mathbb{R}$ correlation function. Typically, δ_i may be set to the range of variation of x_i , so that the condition $\alpha \leq 1$ is ensured. Choosing r as the generalized exponential correlation, we have:

$$\alpha_{\text{exp}}(x_i, c_i) = 1 - \exp \left[- \left(\frac{|x_i - c_i|}{\theta_i} \right)^d \right], \quad (9)$$

with θ_i and d positive parameters to be tuned.

Figure 2 shows a 2D rectangular space distorted by three warpings, when the invariance is on a boundary of x_1 . Figure 3 shows (unconditional) realizations of GPs with a Gaussian kernel applied on the warped space. We see that the invariance at x_1 maximum is ensured. The linear warping induces a strong anisotropy, while with the two other warpings, the process seems stationary far from the critical value.

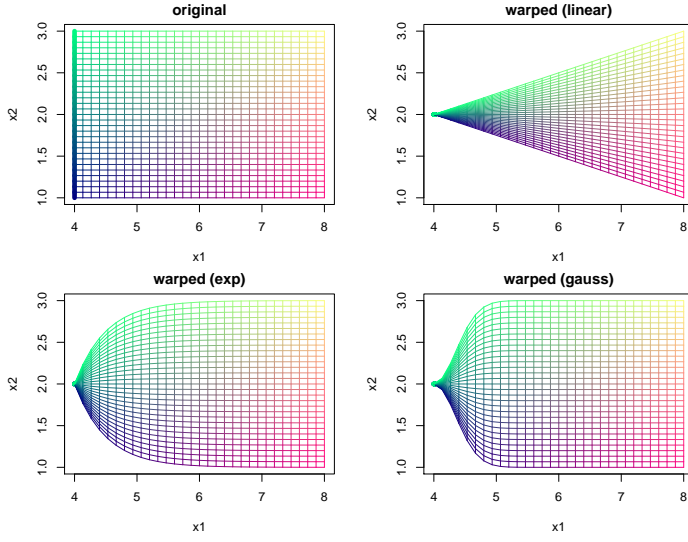


Fig. 2 Three deformations of a 2D space. The local invariance is at $x_1 = 0$, highlighted with larger lines.

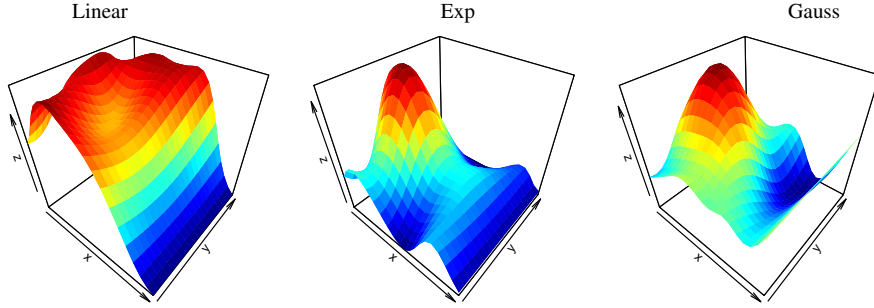


Fig. 3 Three GP realizations using warping functions as shown previously.

3.3.4 Warping for linear invariances

For simplicity, we consider first the particular linear case where $\mathbf{A} = \mathbb{I}_p$ and $\mathbf{b} = \mathbf{c}_I$, that is where invariances occur when a set of variables takes simultaneously a set of critical values: $\mathbf{x}_I = \mathbf{c}_I$. In that case, a possible warping is:

$$\forall j \in J, \quad \tilde{x}_j = \bar{x}_j + (x_j - \bar{x}_j) \alpha_I(\mathbf{x}_I, \mathbf{c}_I). \quad (10)$$

with α_I now a multivariate attenuation function ($\mathbb{R}^{\text{Card}(I)} \times \mathbb{R}^{\text{Card}(I)} \rightarrow \mathbb{R}$), so that, similarly to the simple case:

1. $\alpha_I(\mathbf{c}_I, \mathbf{c}_I) = 0$;
2. α_I increases monotonically with $d(\mathbf{x}_I, \mathbf{c}_I)$ (for some distance $d(., .)$);
3. $0 < \alpha_I \leq 1, \forall \mathbf{x}_I \neq \mathbf{c}_I$.

As in the simple case, linear and correlation-based warpings can be defined as:

$$\alpha_{\text{lin}}(\mathbf{x}_I, \mathbf{c}_I) = \frac{1}{\text{Card}(I)} \sum_{i \in I} \frac{|x_i - c_i|}{\delta_i}, \quad (11)$$

$$\alpha_{\text{cor}}(\mathbf{x}_I, \mathbf{c}_I) = 1 - r_I(\mathbf{x}_I, \mathbf{c}_I), \quad (12)$$

with r_I a $\mathbb{R}^{\text{Card}(I)} \times \mathbb{R}^{\text{Card}(I)} \rightarrow \mathbb{R}$ correlation function as in 9.

Generalizing to the affine case $\mathbf{Ax}_I = \mathbf{b}$, the warping function is the same as in Equation 10, with now:

$$\alpha(\mathbf{x}_I, \mathbf{c}_I) = 1 - r_A(\mathbf{Ax}_I, \mathbf{b}). \quad (13)$$

Figure 4 shows two deformations of the unit cubic space when y is invariant w.r.t. x_3 when 1- $x_1 = x_2 = 0$, and 2- $x_1 = x_2$. On both cases a Gaussian warping (exponential with $d = 2$) is applied.

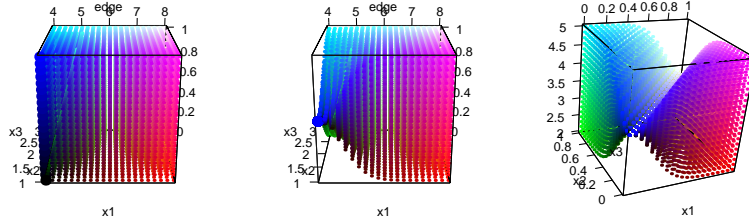


Fig. 4 Left: original space (with the critical edge highlighted). Centered: warping for $c_1 = 0$ AND $c_2 = 1$. Right: warping for $x_1 = x_2$.

3.3.5 Combining warpings

Independent conditions Now, we consider that we have a series of invariance conditions, defined with respect to sets I_1, \dots, I_n and corresponding J_1, \dots, J_n . If $J_k \cap J_l = \emptyset$, $1 \leq j \neq k \leq n$ and $I_i \cap J_k = \emptyset$, $1 \leq j, k \leq n$, the set of warped variables are distinct from the set on which the conditions are written, the invariance conditions are written only once for each variable. In that case, the warpings can be applied independently.

Combinations of simple conditions: “OR” invariance Now, we consider the case when y is invariant w.r.t. a set \mathbf{x}_J for different conditions on sets I_1, \dots, I_n (that, for $\mathbf{x}_{I_1} = \mathbf{c}_{I_1}$ OR $\mathbf{x}_{I_2} = \mathbf{c}_{I_2}$ OR ...). If $J \cap I_i = \emptyset$, $1 \leq i \leq n$, the warping function we propose is:

$$\forall j \in J, \quad \tilde{x}_j = \bar{x}_j + (x_j - \bar{x}_j) \prod_{I \in \{I_1, \dots, I_n\}} \alpha_I(\mathbf{x}_I, \mathbf{c}_I). \quad (14)$$

We see directly that the product of α 's ensure that $\tilde{x}_j = \bar{x}_j$ if any $x_i = c_i$, and the distortion reduces only when *all* the x_i 's are far from the c_i 's. Figure 5 shows a deformation of a cubic space when x_3 is not influent when x_1 or x_2 are minimal, when a Gaussian warping (exponential with $d = 2$) is applied.

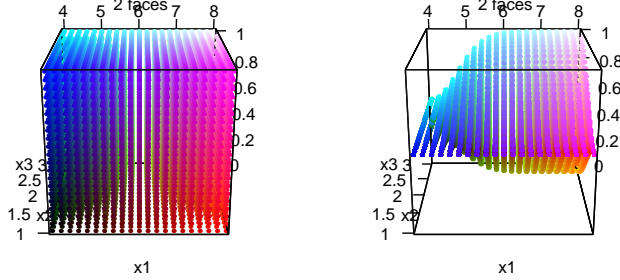


Fig. 5 Warping for $c_1 = 4$ (left face of the cube) OR $c_2 = 1$ (front face). Left: original space, right: distorted space.

“Circular” conditions Difficulty only arises when some variables appear in both I_l 's and J_m 's sets. Take for instance a “reciprocal” condition, e.g., y is invariant w.r.t. \mathbf{x}_J when $\mathbf{x}_I = \mathbf{c}_I$, and invariant w.r.t. \mathbf{x}_I when $\mathbf{x}_J = \mathbf{c}_J$. In that case, applying independently warping functions would lead to:

$$\begin{aligned} \psi(\mathbf{c}_I, \mathbf{x}_J, \mathbf{x}_{-IJ}) &= (\mathbf{c}_I, \bar{\mathbf{x}}_J, \mathbf{x}_{-IJ}), \\ \psi(\mathbf{x}_I, \mathbf{c}_J, \mathbf{x}_{-IJ}) &= (\bar{\mathbf{x}}_I, \mathbf{c}_J, \mathbf{x}_{-IJ}), \\ \text{but: } \psi(\mathbf{c}_I, \mathbf{c}_J, \mathbf{x}_{-IJ}) &= (\mathbf{c}_I, \mathbf{c}_J, \mathbf{x}_{-IJ}), \end{aligned}$$

which induces a discontinuity.

In that case, a simple solution is to fix the non influent variable to its critical value instead of its average, hence applying:

$$\forall k \in K = (\cup_{1 \leq l \leq n} I_l) \cap (\cup_{1 \leq m \leq n} J_m), \quad \tilde{x}_k = c_k + (x_k - c_k) \prod_{i \in I_k} \alpha(x_i, c_i) \quad (15)$$

Remark This formula does not apply in the affine case (Equation 13).

We first show the deformations on a 2D space on Figure 6, where the two critical values are on the boundaries of x_1 and x_2 . Here, the warping of Equation 15 is applied on each variable ($K = \{1, 2\}$). Again, except for the linear warping, the local topology is preserved far from the critical edges.

As another illustrative example, we consider a cubic space with the following circular conditions:

- y is invariant w.r.t. x_2 if $x_1 = 4$;

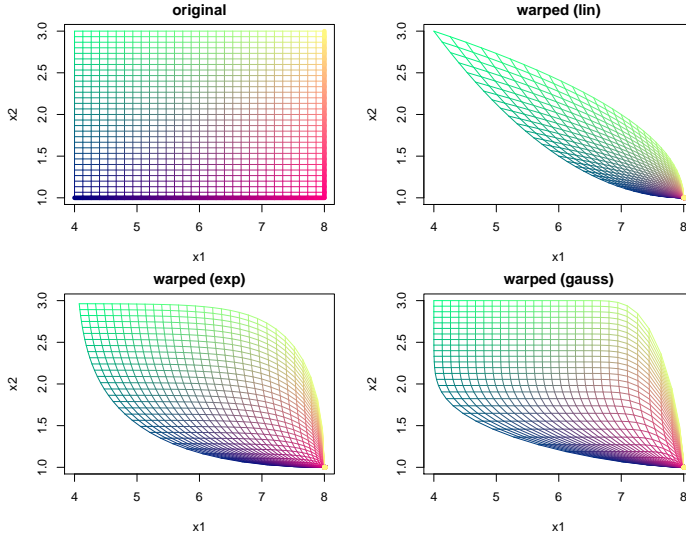


Fig. 6 Three deformations of a 2D space, with invariance at $x_1 = 8$ OR $x_2 = 1$, highlighted with larger lines.

- y is invariant w.r.t. x_3 if $x_2 = 1$;
- y is invariant w.r.t. x_1 if $x_3 = 0$.

All critical values correspond to the lower bounds of the variables. Equation 15 is applied to each variable, hence with $K = \{1, 2, 3\}$, $C = [4, 1, 0]$ and $I_1 = 3$, $I_2 = 1$, and $I_3 = 2$. The original and distorted space is shown in Figure 7.

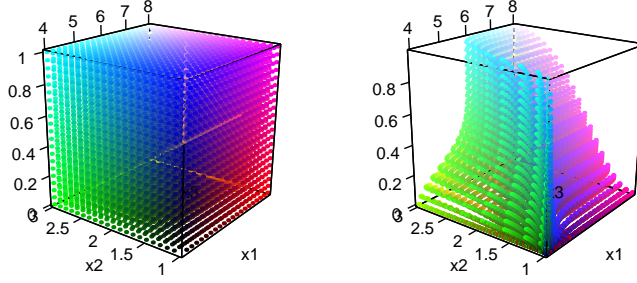


Fig. 7 Warping with circular conditions. Left: original space, right: distorted space.

3.3.6 Warping parameters tuning

The linear warping has the advantage of being parameter-free, which comes at a price of a profound modification of the problem topology. The correlation-based warpings

have the capability of creating more localized distortions, but depend on range parameters (the θ_i 's in Equation 9). Those may be estimated by likelihood maximization along with the GP covariance parameters [30, 13].

However, we found in our numerical experiments that choosing the same correlation function for the GP and the warping, and fixing the warping ranges to be 1/10th of the GP ones provided very satisfactory results, while avoiding the extra computational burden.

Note that in the case of linear invariances, choosing the range of the correlation r_A is non-trivial, as it is not directly linked to design variables. A possible solution is $\theta_A = \mathbf{A}^T \theta_I$.

4 A warping-based Bayesian optimization of the Sharka model

4.1 Numerical setup

4.1.1 Experiments description

To evaluate the benefits of including the warping step in the optimization process (i.e. reducing the parameter space removing the combinations which lead to the same management), we conducted 50 independent optimizations of sharka management parameters with and without the warping step. The criterion to optimize was the mean of the NPV (\overline{NPV}). For this to happen, we randomly selected 50 times 200 management strategies using a maximin Latin hypercube sampling design [7]. Then, for each sampling design of 200 strategies, we performed 2 optimizations in parallel: with and without the warping step. For one optimization, we performed sequentially 200 iterations allowing to choose 200 new strategies, resulting in a total of 400 evaluated strategies. These 200 new strategies were selected each time among 100,000 randomly generated candidate points over the parameter space and 10,000 more locally around the best point found. In addition, for each evaluated strategy, 1000 simulations were carried out (with different random seed) to take into account the variability due to the epidemic and landscape characteristics.

4.1.2 Bayesian optimization setup

For all experiments, we used the same GP modeling setup, that is, an unknown constant trend (ordinary kriging, [14]) and Matern 5/2 covariance function [22, Chapter 4]. The acquisition function maximized at each step is the expected improvement on the *reinterpolating* model. The maximization is performed by a large-scale random search followed by a local optimization starting for the optimum found by the random search. All experiments were conducted in R [21], using code adapted from the DiceOptim package [18].

4.1.3 Comparison metrics

We firstly compared the optimization results by subtracting the \overline{NPV} achieved using the optimization with the warping step and the optimization without the warping step (obtained from the same sampling design).

In addition, we compared the optimization speed between the optimizations with or without warping. To this end, we used two different ways. Firstly, we performed a nonlinear regression of \overline{NPV} obtained for all the selected strategies during the optimization process with and without the warping step, and we compared the growth parameter c of the following regression: $a + b \times \exp^{-c \times x}$.

Secondly, we used a specific algorithm developed by [Coralie's comment: reference???]. Briefly, we uniformly defined 100 α values between a minimum and a maximum values. Then, for each iteration performed in the optimization process (i.e. for each of the 200 evaluated strategies), we add: the number of optimizations (under 50) which exceed α 1, the number of optimizations which exceed α 2, ..., the number of optimizations which exceed α 100. We used $\alpha \in [0;18,012.12]$, and then $\alpha \in [10,000;18,012.12]$. The value 18,012.12 corresponds to the maximal value of \overline{NPV} identified in all the optimizations.

4.2 Results and insights into the Sharka model

We firstly subtracting the \overline{NPV} obtained with optimizations with and without the warping step. In 24 out of the 50 optimization cases, we obtained better \overline{NPV} with the warping step than without (Fig.8). This result means that with 200 iterations in the optimization, the final optimization result is not impacted by the use of a warping step.

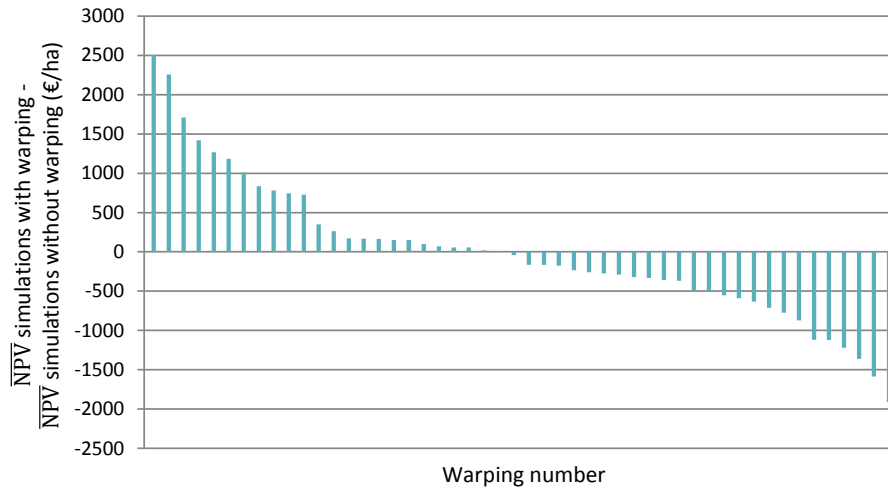


Fig. 8 Comparison of \overline{NPV} obtained at the end of the optimization with and without warping.

However, we showed that the warping can impact the optimization speed (Fig.9). Indeed, the parameter c corresponding to the growth parameter of a nonlinear regression was higher with (0.26) than without (0.18) warping (Fig.10). In addition, we can visually observe that the warping step allow to improve the optimization speed on the Fig.11 and 12 which present the results of the algorithm developed by [Coralie's comment: reference??].

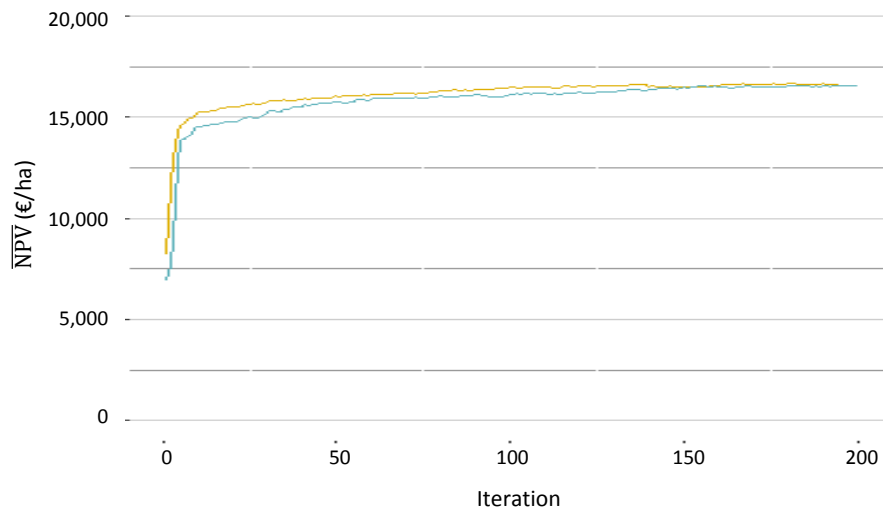


Fig. 9 Comparison of \overline{NPV} obtained during optimizations with and without warping. Yellow and blue lines represent the mean of the \overline{NPV} selected at each iteration for the 50 optimizations respectively performed with and without the warping step.

5 Conclusion

In this study, we showed how a Bayesian optimization process can be improved accounting for the parameter invariances. These invariances correspond to the insensitivity of the model to a subset of parameters for some values of another subset of parameters. Here, we take as an example the optimization problem of sharka control. In our study, we used a spatiotemporal model simulating sharka management characterized by 10 parameters related to the surveillance of the orchards. In this example, the invariances arise because parameters (radius of different zones, surveillance frequency in each zone, detection probability of infected trees, and duration of observation zones) are strongly related. Indeed, we easily note, for instance, that when the detection probability takes a value of 0, numerous other parameters do not influence the model results. Firstly, we presented how we took into account such invariances in the Bayesian optimization process with the warping. Then, we applied this process to the sharka model in order to analyze the warping efficiency.

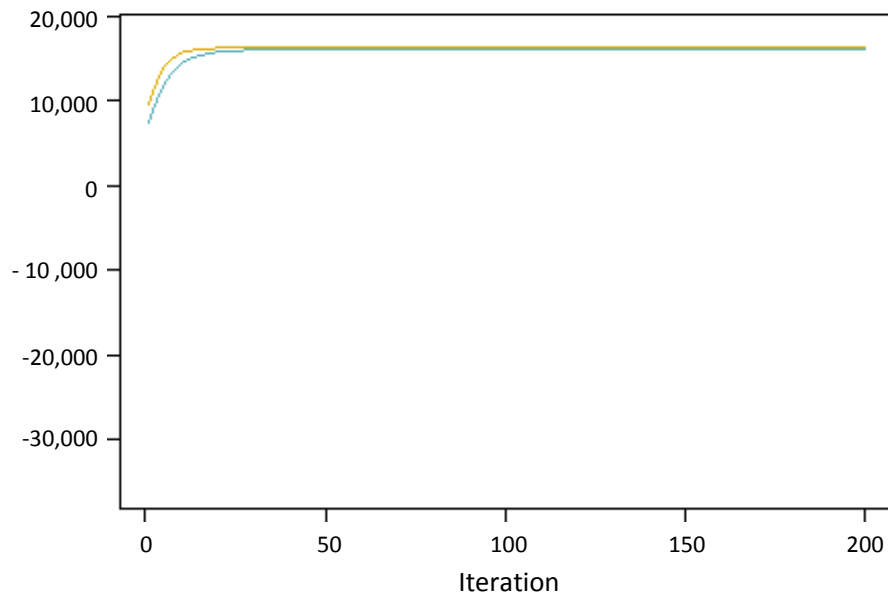


Fig. 10 Non linear regression on \overline{NPV} obtained at each iteration of the optimizations with (yellow) and without (blue) warping.

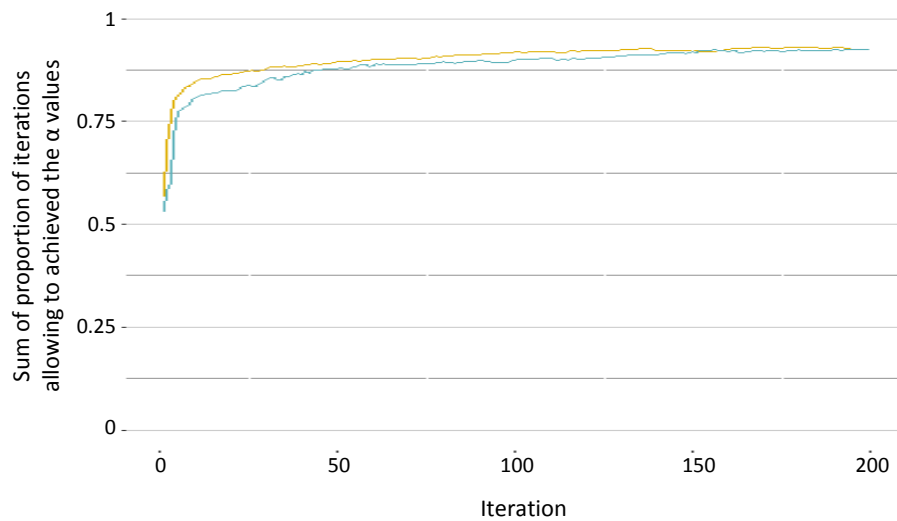


Fig. 11 Results of the Coco algorithm with (yellow) and without (blue) warping ($\alpha \in [0;18,012.12]$).

5.1 Bayesian optimization and warping strategy

In order to tackle invariances due to the management parameters, we adapted a Bayesian optimization process including warping conditions to the parameter space. [Coralie's

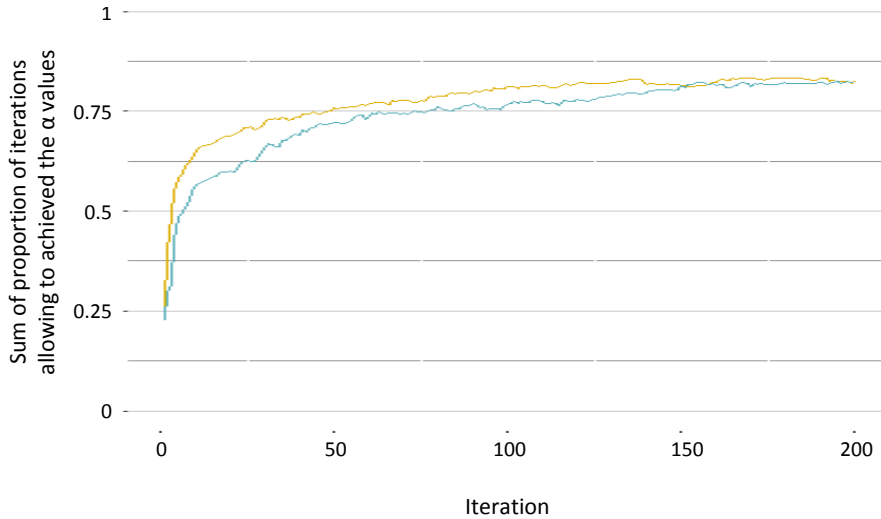


Fig. 12 Results of the Coco algorithm with (yellow) and without (blue) warping ($\alpha \in [10,000; 18,012.12]$).

comment: peut etre a etoffer] We applied this Bayesian optimization process to the spatio temporal sharka model. We performed various optimizations of its management parameters firstly with the use of warping (which allows accounting for the invariances) and then without. We showed that the optimization results are not impacted by the use of the warping. This means that if the optimization process includes enough iterations, the warping does not improve the result. Nevertheless, the optimization speed was impacted: the optimization process with warping was faster than without. This shows that we could perform less iterations to obtain the same result, which means we could save time.

Thus, in order to reduce the calculation time, such warping approach could be used for various optimization issues presenting invariances. For instance, we could use it to optimize all management parameters included in the spatio temporal sharka model developed by Rimbaud et al. [25] (here, we optimized only 10 out of 23 management parameters included in the model). Nevertheless, it may be difficult to define the minimum number of iteration to perform to reach the optimal value. However, the warping use cannot affect negatively the optimization performance. Indeed, if numerous iterations are performed, the warping use will probably be unnecessary. Conversely, if the number of iterations is limited, the warping can allow obtaining better results.

5.2 Possible extensions

References

References

1. Bajardi P, Barrat A, Savini L, Colizza V (2012) Optimizing surveillance for live-stock disease spreading through animal movements. *Journal of the Royal Society Interface* 9(76):2814–2825
2. Box GE, Draper NR (1987) Empirical model-building and response surfaces. John Wiley & Sons
3. Cambra M, Capote N, Myrta A, Llácer G (2006) Plum pox virus and the estimated costs associated with sharka disease. *EPPO Bulletin* 36(2):202–204
4. Cunniffe NJ, Koskella B, Metcalf CJ, Parnell S, Gottwald TR, Gilligan CA (2015) Thirteen challenges in modelling plant diseases. *Epidemics* 10:6–10
5. Cunniffe NJ, Cobb RC, Meentemeyer RK, Rizzo DM, Gilligan CA (2016) Modeling when, where, and how to manage a forest epidemic, motivated by sudden oak death in California. *Proceedings of the National Academy of Sciences* 113(20):5640–5645
6. Duvenaud D (2014) Automatic model construction with gaussian processes. PhD thesis, University of Cambridge
7. Fang KT, Li R, Sudjianto A (2005) Design and modeling for computer experiments. Chapman and Hall/CRC
8. Ginsbourger D, Durrande N, Roustant O (2013) Kernels and designs for modelling invariant functions: From group invariance to additivity. In: mODa 10—Advances in Model-Oriented Design and Analysis, Springer, pp 107–115
9. Grechi I, Ould-Sidi MM, Hilgert N, Senoussi R, Sauphanor B, Lescourret F (2012) Designing integrated management scenarios using simulation-based and multi-objective optimization: Application to the peach tree–*myzus persicae* aphid system. *Ecological Modelling* 246:47–59
10. J Forrester AI, Keane AJ, Bressloff NW (2006) Design and analysis of “noisy” computer experiments. *AIAA journal* 44(10):2331–2339
11. Jones DR, Schonlau M, Welch WJ (1998) Efficient global optimization of expensive black-box functions. *Journal of Global Optimization* 13(4):455–492
12. Kompas T, Ha PV, Nguyen HTM, East I, Roche S, Garner G (2017) Optimal surveillance against foot-and-mouth disease: the case of bulk milk testing in Australia. *Australian Journal of Agricultural and Resource Economics* 61(4):515–538
13. Marmin S, Ginsbourger D, Baccou J, Liandrat J (2018) Warped gaussian processes and derivative-based sequential designs for functions with heterogeneous variations. *SIAM/ASA Journal on Uncertainty Quantification* 6(3):991–1018
14. Matheron G (1963) Principles of geostatistics. *Economic Geology* 58(8):1246–1266
15. Mockus J (2012) Bayesian approach to global optimization: theory and applications, vol 37. Springer Science & Business Media

16. Mushayabasa S, Tapedzesa G (2015) Modeling the effects of multiple intervention strategies on controlling foot-and-mouth disease. *BioMed research international* 2015
17. Picard C, Samuel S, Jacquot E, Thébaud G (2018) Analyzing the influence of landscape aggregation on disease spread to improve management strategies. (in prep)
18. Picheny V, Ginsbourger D (2014) Noisy kriging-based optimization methods: a unified implementation within the diceoptim package. *Computational Statistics & Data Analysis* 71:1035–1053
19. Picheny V, Wagner T, Ginsbourger D (2013) A benchmark of kriging-based infill criteria for noisy optimization. *Structural and Multidisciplinary Optimization* 48(3):607–626
20. Pleydell DR, Soubeyrand S, Dallot S, Labonne G, Chadœuf J, Jacquot E, Thébaud G (2018) Estimation of the dispersal distances of an aphid-borne virus in a patchy landscape. *PLoS computational biology* 14(4):e1006,085
21. R Core Team (2018) R: A Language and Environment for Statistical Computing. R Foundation for Statistical Computing, Vienna, Austria, URL <https://www.R-project.org/>
22. Rasmussen CE, Williams C (2006) Gaussian Processes for Machine Learning. MIT Press, URL <http://www.gaussianprocess.org/gpml/>
23. Rimbaud L, Dallot S, Gottwald T, Decroocq V, Jacquot E, Soubeyrand S, Thébaud G (2015) Sharka epidemiology and worldwide management strategies: learning lessons to optimize disease control in perennial plants. *Annual review of phytopathology* 53:357–378
24. Rimbaud L, Bruchou C, Dallot S, Pleydell DR, Jacquot E, Soubeyrand S, Thébaud G (2018) Using sensitivity analysis to identify key factors for the propagation of a plant epidemic. *Royal Society open science* 5(1):171,435
25. Rimbaud L, Dallot S, Bruchou C, Thoyer S, Jacquot E, Soubeyrand S, Thébaud G (2018) Heuristic optimisation of the management strategy of a plant epidemic using sequential sensitivity analyses. *bioRxiv* p 315747
26. Rios LM, Sahinidis NV (2013) Derivative-free optimization: a review of algorithms and comparison of software implementations. *Journal of Global Optimization* 56(3):1247–1293
27. Roustant O, Ginsbourger D, Deville Y (2012) DiceKriging, DiceOptim: Two R packages for the analysis of computer experiments by kriging-based meta-modeling and optimization. *Journal of Statistical Software* 51(1):1–55, URL <http://www.jstatsoft.org/v51/i01/>
28. Shahriari B, Swersky K, Wang Z, Adams RP, De Freitas N (2016) Taking the human out of the loop: A review of bayesian optimization. *Proceedings of the IEEE* 104(1):148–175
29. Snelson E, Ghahramani Z, Rasmussen CE (2004) Warped gaussian processes. In: *Advances in neural information processing systems*, pp 337–344
30. Snoek J, Swersky K, Zemel R, Adams R (2014) Input warping for bayesian optimization of non-stationary functions. In: *International Conference on Machine Learning*, pp 1674–1682

31. Tildesley MJ, Savill NJ, Shaw DJ, Deardon R, Brooks SP, Woolhouse ME, Grenfell BT, Keeling MJ (2006) Optimal reactive vaccination strategies for a foot-and-mouth outbreak in the uk. *Nature* 440(7080):83
32. VanderWaal K, Enns EA, Picasso C, Alvarez J, Perez A, Fernandez F, Gil A, Craft M, Wells S (2017) Optimal surveillance strategies for bovine tuberculosis in a low-prevalence country. *Scientific reports* 7(1):4140